ISSN 1070-3284, Russian Journal of Coordination Chemistry, 2014, Vol. 40, No. 5, pp. 259–267. © Pleiades Publishing, Ltd., 2014.
Original Russian Text © P.A. Abramov, A.V. Rogachev, M.A. Mikhailov, A.V. Virovets, E.V. Peresypkina, M.N. Sokolov, V.P. Fedin, 2014, published in Koordinatsionnaya Khimiya, 2014, Vol. 40, No. 5, pp. 259–268.

# Hexanuclear Chloride and Brimode Tungsten Clusters and Their Derivatives[1]

**P. A. Abramov[a, b, *], A. V. Rogachev[a], M. A. Mikhailov[a], A. V. Virovets[a], E. V. Peresypkina[a], M. N. Sokolov[a, b], and V. P. Fedin[a, b]**

[a] *Nikolaev Institute of Inorganic Chemistry, Siberian Branch of Russian Academy of Sciences, Novosibirsk, Russia*
[b] *Novosibirsk State University*
**e-mail: abramov@niic.nsc.ru*

Received August 28, 2013

**Abstract**—Several hexanuclear chloride and bromide bridged tungsten clusters have been prepared. Two new oxo-bridged clusters, $Na[W_6OBr_{18}]$ and $[\alpha\text{-}W_6(\mu_2\text{-}OH)_4(\mu_2\text{-}O)_6(\mu_2\text{-}Cl)_2Cl_6]^{2-}$ are reported. Crystal structures of eight new tungsten cluster complexes with different core types were determined. The possibility of Se for Cl substitution in the $\{W_6Cl_8\}^{4+}$ core was investigated.

**DOI:** 10.1134/S1070328414050017

## INTRODUCTION

Clusters of 5–7 group transition metals with $\{M_6(\mu_3\text{-}X)_8\}^{n+}$ (M = Nb, Mo, W, Tc, Re; X—halogen or chalcogen atom) core form an extensive family of high-valence inorganic cluster compounds [1, 2]. This family also includes Chevrel phases ($PbMo_6S_8$ etc.) with thermoelectric and superconducting properties [3–6]. The molecular clusters of this family are attractive candidates for design of solar energy converting systems because of their prominent photophysical and redox properties [2, 7]. Specifically, luminescence of this compounds can be used for energy transmission and triplet-singlet oxygen conversion [1]. Molybdenum clusters are better studied [2–8] compared to the tungsten analogues. In this work report preparation and structural characterization of a number of new salts with $[W_6X_{14}]^{2-}$ (X = Cl, Br) anion, the perfluorobutyrate complex $(Bu_4N)_2[W_6Cl_8(C_3F_7COO)_6]$ and new oxo-halide clusters $(Bu_4N)_2[\alpha\text{-}W_6(\mu_3\text{-}O)_6(\mu_3\text{-}Cl)_6Cl_6]$, $(PyH)_2[\alpha\text{-}W_6(\mu_2\text{-}OH)_4(\mu_2\text{-}O)_6(\mu_2\text{-}Cl)_2Cl_6]$ and $Na[W_6OBr_{18}]$. The possibility of bridging chloride substitution in $\{W_6(\mu_3\text{-}Cl)_8\}^{4+}$ core with selenide was also explored.

## EXPERIMENTAL

All reagents were commercially available and used as purchased without further purification. Solvents were purified by standard procedures. Reactions involving $H_2Se$ were handled in a well-ventilated fume cupboard. The ampoules (200 × 20 mm) were opened after cooling with liquid $N_2$. IR spectra were recorded with a Scimitar FTS 2000 spectrometer. ESI–MS spectra were recorded with a Quattro LC (Micromass, Manchester, UK). Sample solutions were injected through injection pump at 6 L/min rate. The capillary voltage was 3.5 kV, the chamber voltage varied between –10 and –60 V. Formulated composition of every peak was compared with theoretically predicted isotopic pattern using MassLynx 3.5 (MassLynx 3.5; Micromass: Manchester, UK, 1998). Elemental analysis was carried out in the analytic service of NIIC SB RAS.

**X-ray structure analysis.** Crystallographic characteristics of compounds and experiment details are listed in Table 1. The data were collected on a single-crystal diffractometer Bruker X8Apex CCD ($MoK_\alpha$, $\lambda = 0.71073$ Å) by standard scanning of narrow (0.5°) frames at 100 K. The structures were solved directly and refined by full-matrix least-squares treatment on $|F_{obs}|^2$ in anisotropic approximation using SHELXTL program set [9]. Absorption correction was applied with SADABS program [10]. Hydrogen atoms were placed in their geometrically calculated positions and refined using riding model. Packing of cluster anions in the crystal structures was analyzed with TOPOS 4.0 Professional program [11]. Atom coordinates have been deposed with The Cambridge Crystallographic Data Centre under deposition numbers 889201–889205 (available by request at http://www.ccdc.cam.ac.uk), and in Fachinformationszentrum Karlsruhe, 76344 Eggenstein-Leopoldshafen, Germany (fax: (+49) 7247-808-666; e-mail: crysdata@fiz-karlsruhe.de) under numbers 424877, 424892, and 424893.

**$(Bu_4N)_2[W_6Cl_{14}]$ (I) and $(Bu_4N)_2[\alpha\text{-}W_6(\mu_2\text{-}O)_6(\mu_2\text{-}Cl)_6Cl_6]$ (II):** The reduction of $WCl_6$ with metallic antimony in the presence of NaCl was carried out as reported in [12], but the crude melt was then treated in air. Extraction with HCl gives a yellow-green solution, which after addition of 1.5 g $Bu_4NBr$

---

[1] The article was translated by the authors.

**Table 1.** X-ray experiments details

| Parameter | Value | | | | | | | |
|---|---|---|---|---|---|---|---|---|
| | **I** | **II** | **IV** | **V** | **VI** | **VII** | **VIII** | **IX** |
| $M$ | 2084.32 | 2109.42 | 1876.48 | 1783.01 | 3149.86 | 2804.51 | 2580.47 | 2244.83 |
| Crystal system, space group | Monoclinic, $P2_1/n$ | Triclinic, $P\bar{1}$ | Hexagonal, $P\bar{3}1c$ | Orthorhombic, $Pnnm$ | Monoclinic, $P2_1/n$ | Triclinic, $P\bar{1}$ | Hexagonal, $P6_3/m$ | Cubic, $Pn\bar{3}$ |
| Temperature, K | 100 | 100 | 203 | 296 | 100 | 150 | 150 | 150 |
| $a$, Å | 12.6300(11) | 12.5619(2) | 9.7941(6) | 9.1567(3) | 12.4215(3) | 13.5580(4) | 9.3827(2) | 13.4289(2) |
| $b$, Å | 11.4734(10) | 12.9716(3) | 9.7841(6) | 12.7498(4) | 17.9360(6) | 15.0908(4) | 9.3827(2) | 13.4289(2) |
| $c$, Å | 18.5232(14) | 19.6207(4) | 14.329(2) | 13.3445(4) | 20.1925(6) | 16.7646(5) | 18.3342(5) | 13.4289(2) |
| $\alpha$, deg | 90 | 87.459(1) | 90 | 90 | 90 | 69.461(1), | 90 | 90 |
| $\beta$, deg | 90.022(4) | 74.301(1) | 90 | 90 | 103.296(1) | 72.185(1), | 90 | 90 |
| $\gamma$, deg | 90 | 63.793(1) | 120 | 90 | 90 | 67.048(1) | 120 | 90 |
| $V$, Å$^3$ | 2684.2(4) | 2751.02(10) | 1190.4(2) | 1557.92(8) | 4378.1(2) | 2900.28(14) | 1397.81(6) | 2421.71(6) |
| $Z$ | 2 | 2 | 2 | 2 | 2 | 2 | 2 | 4 |
| $F(000)$ | 1920 | 1948 | 1597 | 1752 | 2952 | 2504 | 2186 | 3780 |
| $\mu$, mm$^{-1}$ | 13.53 | 13.11 | 33.45 | 23.634 | 8.24 | 21.55 | 50.33 | 51.49 |
| Crystal size (mm) | 0.12 × 0.06 × 0.05 | 0.21 × 0.12 × 0.10 | 0.10 × 0.03 × 0.02 | 0.07 × 0.06 × 0.03 | 0.53 × 0.06 × 0.05 | 0.20 × 0.20 × 0.20 | 0.29 × 0.25 × 0.04 | 0.30 × 0.04 × 0.03 |
| $T_{min}$, $T_{max}$ | 0.335, 0.508 | 0.024, 0.269 | 0.135, 0.554 | 0.735, 1 | 0.488, 0.662 | 0.654, 1 | 0.005, 0.158 | 0.023, 0.307 |
| No of measured, independent and observed ($I > 2\sigma(I)$) reflections | 17261/5909/3800 | 22548/9349/8095 | 3336/845/533 | 10774/2631/2261 | 47086/12741/9872 | 36179/15824/11678 | 17623/2461/1916 | 18146/1010/949 |
| $R_{int}$ | 0.066 | 0.028 | 0.064 | 0.020 | 0.056 | 0.034 | 0.114 | 0.033 |
| $\theta_{max}$, deg | 27.5 | 25.0 | 28.3 | 33.43 | 32.0 | 31.7 | 37.6 | 28.3 |
| $h, k, l$ ranges | $-15 \le h \le 15$,<br>$-14 \le k \le 14$,<br>$-24 \le l \le 16$ | $-14 \le h \le 14$,<br>$-15 \le k \le 15$,<br>$-23 \le l \le 23$ | $-10 \le h \le 12$,<br>$-11 \le k \le 8$,<br>$-18 \le l \le 12$ | $-13 \le h \le 13$,<br>$-18 \le k \le 15$,<br>$-12 \le l \le 19$ | $-17 \le h \le 14$,<br>$-24 \le k \le 26$,<br>$-29 \le l \le 29$ | $-19 \le h \le 19$,<br>$-16 \le k \le 21$,<br>$-22 \le l \le 23$ | $-16 \le h \le 14$,<br>$-14 \le k \le 16$,<br>$-30 \le l \le 14$ | $-17 \le h \le 15$,<br>$-17 \le k \le 16$,<br>$-17 \le l \le 14$ |
| $R(F^2 > 2\sigma(F^2))$, $wR(F^2)$ | 0.058, 0.131 | 0.030, 0.070 | 0.064, 0.173 | 0.0364, 0.1142 | 0.047, 0.064 | 0.027, 0.050 | 0.028, 0.057 | 0.018, 0.050 |
| GOOF | 1.09 | 1.06 | 1.11 | 1.124 | 1.04 | 0.98 | 1.03 | 1.46 |
| No of parameters, restraints | 257, 0 | 523, 0 | 38, 0 | 96, 0 | 572, 0 | 620, 12 | 45, 0 | 33, 0 |
| Weighting scheme | $w = 1/[\sigma^2(F_o^2) + (0.0147P)^2 + 126.2823P]$, where $P = (F_o^2 + 2F_c^2)/3$ | $w = 1/[\sigma^2(F_o^2) + (0.0243P)^2 + 23.6514P]$, where $P = (F_o^2 + 2F_c^2)/3$ | $w = 1/[\sigma^2(F_o^2) + (0.0461P)^2 + 193.156P]$, where $P = (F_o^2 + 2F_c^2)/3$ | $w = 1/[\sigma^2(F_o^2) + (0.0125P)^2 + 1.2P]$, where $P = (F_o^2 + 2F_c^2)/3$ | $w = 1/[\sigma^2(F_o^2) + (0.0123P)^2 + 10.4412P]$, where $P = (F_o^2 + 2F_c^2)/3$ | $w = 1/[\sigma^2(F_o^2) + (0.P)^2]$, where $P = (F_o^2 + 2F_c^2)/3$ | $w = 1/[\sigma^2(F_o^2) + (0.0073P)^2]$, where $P = (F_o^2 + 2F_c^2)/3$ | $w = 1/[\sigma^2(F_o^2) + (0.0167P)^2 + 17.9257P]$, where $P = (F_o^2 + 2F_c^2)/3$ |
| $\Delta\rho_{max}/\Delta\rho_{min}$, $e$ Å$^{-3}$ | 4.86/–2.81 | 2.80/–2.01 | 2.46/–6.18 | 2.527/–3.416 | 1.96/–1.47 | 1.10/–1.11 | 4.48/–3.12 | 0.89/–2.26 |

* Computer programs: Apex2 V.1.27 (Bruker, 2005), SHELXS97 (Sheldrick, 1990), SHELXL97 (Sheldrick, 1997), SHELXTL V6.22 (Bruker, 2000–2005).

gives a yellow-orange precipitate. The precipitate was filtered, dried in vacuo and dissolved in 20 mL of $CH_3CN$. Slow diffusion of diethyl ether vapor at 4°C yielded a mixture of yellow (**I**) and red (**II**) crystals in two days, suitable for X-ray analysis. Complex **I** was also prepared quantitatively by reaction of **III** with $Bu_4NBr$ in HCl. Calculated for $(Bu_4N)_2[W_6Cl_{14}]$ : C : H : N (%) 18.8 : 3.7 : 1.3; found: 18.4 : 3.5 : 1.3.

**$(H_7O_3)_2[W_6Cl_{14}] \cdot 3H_2O$ (III):** 4.3 g of metallic Bi (0.02 mol) and 8.8 g of $WCl_6$ (0.022 mol) were placed into a glass ampoule, which was evacuated and sealed. The mixture was heated at 230°C, for 2 h, and at 355°C for another 2 hours, and then the ampoule was placed in a temperature gradient such as its empty end was situated in the cooler part of the furnace, and heated at 350°C for 24 hours. After cooling to the room temperature the ampoule was opened up gently in order to avoid mixing the dark with $BiCl_3$, sublimated in the cooler end. Then the melt (8.1 g) was washed with 8 mL of cold conc. HCl, filtered through a glass filter, and the dark precipitate was extracted with 15 mL of hot conc. HCl by boiling for 30 min. The insoluble part was removed by filtration. Cooling of the filtrate yielded light yellow crystalline precipitate of $(H_7O_3)_2[W_6Cl_{14}] \cdot 3H_2O$ (**III**) as thin long needles. Yield 4.1 g (65%).

**$Cs_2[W_6Cl_{14}] \cdot 0.63H_2O$ (IV):** A solution of 1.05 g (0.6 mmol) of **III** in 8 mL of conc. HCl was added to a solution of 0.20 g (1.2 mmol) of CsCl in 5 mL of conc. HCl. Yellow crystals of the cesium separated. Yield 79%. Anal. Calc. for Cl 26.4%. Found Cl 26.1%.

**$(PyH)_2[\alpha\text{-}W_6(\mu_2\text{-}OH)_4(\mu_2\text{-}O)_6(\mu_2\text{-}Cl)_2Cl_6] \cdot 4H_2O$ (V):** 0.5 mL of pyridine was added to 5 mL of the brown hydrochloric solution exctract from synthesis of **I** instead of $Bu_4NBr$. A yellow-orange solid precipitated immediately, which was redissolved upon heating and after slow cooling yielded a mixture of yellow and red crystals. Yellow crystals were show to be $(PyH)_2[W_6Cl_{14}]$.

For $C_{10}H_{12}N_2Cl_{14}W_6$

| | | | |
|---|---|---|---|
| anal. calcd., %: | C, 6.84; | H, 0.69; | N, 1.60. |
| Found, %: | C, 7.00; | H, 1.07; | N, 1.44. |

The composition and structure of the red crystals were established by X-ray diffraction (**V**).

**$(Bu_4N)_2[W_6Cl_8(C_3F_7COO)_6]$ (VI):** 10 mL of $CHCl_3$ were added to a mixture of $(Bu_4N)_2[W_6Cl_{14}]$ (0.24 g, 0.12 mmol) and $AgC_3F_7COO$ (0.22 g, 0.69 mmol), and the suspension was stirred mixed in a foil-covered flask for 24 hours. AgCl precipitate was filtered out from yellow solution, and the filtrate was rota-evaporated. Addition of diethyl ether to the oily residue gives pale-yellow crystals of **VI** in two days. Yield 50%. IR (KBr, 4000–400 $cm^{-1}$): 2972 (m), 2884 (w), 1716 (s), 1486 (m), 1366 (m), 1326 (m), 1269 (m), 1213 (s), 1166 (m), 1118 (m), 1080 (m), 966 (m), 931 (m), 881 (w), 807 (m), 738 (m), 714 (w), 598 (w), 527 (w), 492 (w), 438 (w).

**$[Na(diglyme)]_2[W_6Br_{14}]$ (VII):** Tungsten powder (3.50 g, 0.02 mol), NaBr (0.65 g, 6.0 mmol) and 1.0 mL of bromine (0.02 mol) were placed in a quartz ampoule, which was evacuated, sealed, and heated at 720°C for 2 days. After cooling the ampoule was opened and the solidified melt melt was extracted with diglyme (50 mL, 150°C) during 2 days under Ar. The solution was filtered and **VII** was crystallized after layering with diethyl ether as yellow crystalline solid (0.335 g, 10%).

**$Na[W_6OBr_{18}]$ (VIII)**: Tungsten powder, niobium powder, NaBr and bromine (1.0 mL) were placed in a quartz ampoule in 10 : 2 : 6 : 11 molar ratio. The ampoule was evacuated, sealed and heated at 720°C for 2 days. After cooling brown crystals of **VIII** were found on ampoule walls. Formula and structure were determined by X-ray diffraction. Yield 5%. The compound is unstable on humid air because of quick hydrolysis.

**$Na[W_6Br_{14}]$ (IX)**: Tungsten powder, NaBr and bromine (1.0 mL) were placed in a quartz ampoule in 6 : 2 : 6 molar ratio. The ampoule was evacuated, sealed and heated at 720°C for 2 days. After cooling brown crystals of **IX** were found on ampoule walls. Formula and structure were determined by X-ray diffraction. Yield 5%.

**Reaction of III with $H_2Se$ in situ:** 0.9 g (0.5 mmol) of **III**, 0.23 g (1.6 mmol) of ZnSe and 2 mL of 4M HCl were placed into a glass ampoule, which was evacuated, sealed and heated at 150°C for 8 hours. After cooling the ampoule contained an orange-red solution with a small amount of a black precipitate. The precipitate was filtered out and the solution was added to a solution of $Bu_4NBr$ (0.5 g, 1.68 mmol) in 3.0 mL of conc. HCl. Light gray precipitate was filtered out and dried in vacuo. Yield 0.84 g.

For $C_{32}H_{72}N_2Cl_{14}W_6$

| | | | |
|---|---|---|---|
| anal. calcd., %: | C, 18.48; | H, 3.49; | N, 1.35. |
| Found, %: | C, 18.28; | H, 3.44; | N, 1.35. |

IR (KBr, 4000–400 $cm^{-1}$): 3444 (m), 2961 (s), 2873 (s), 1622 (w), 1464 (s), 1381 (m), 1151 (w), 1063 (w), 1023 (w), 973 (w), 881 (w), 813 (w), 738 (w). IR (500–100 $cm^{-1}$): 445 (w), 306 (s), 285 (s), 224 (m), 104 (w). The precipitate was dissolved in 2 mL of $CH_3CN$ and the solution was put into diethyl ether vapor at 4°C. A mixture of yellow and red crystals was obtained. According to ESI–MS(–) in $CH_3CN$, orange crystals contain $[W_6(\mu_3\text{-}SeCl_7)Cl_6]^{2-}$ ($m/z$ = 800) as well as $[W_6(\mu_3\text{-}SeCl_7)Cl_6]^{2-}$ ($m/z$ = 547) in 2 : 1 molar ratio. Determination of crystal parameters shows that yellow crystals are $(NBu_4)_2[W_6Cl_{14}]$ [13].

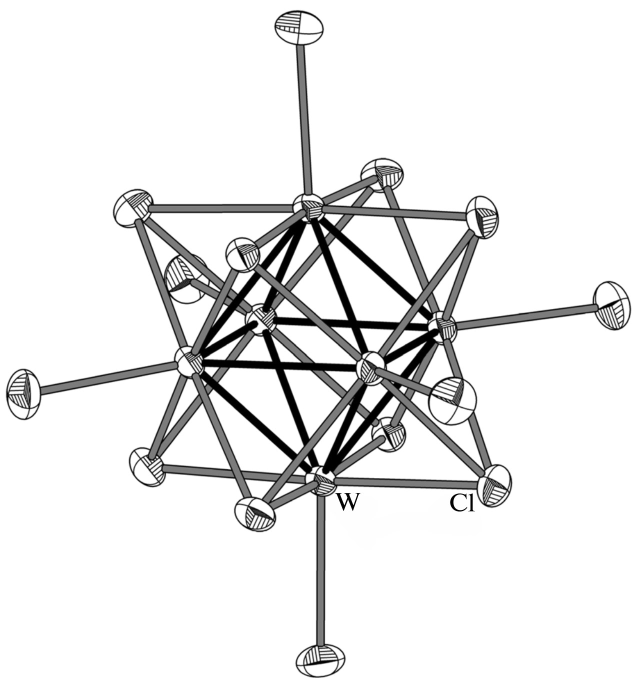

**Fig. 1.** Structure of a $[W_6(\mu_3\text{-}Cl)_8Cl_6]^{2-}$.

## RESULTS AND DISCUSSION

**Synthesis and reaction ability.** Standard approaches to $W_6Cl_{12}$ employ reduction of $WCl_6$ with various metals [12]. It is assumed that the best way consists in the reduction with bismuth in the presence of KCl [12]. In this work we have carried reduction of $WCl_6$ with metallic antimony in presence of NaCl under similar conditions, followed by work-up in air. This procedure yielded a mixture of $Bu_4N^+$ salts of $[W_6Cl_{14}]^{2-}$ (**I**) and $[\alpha\text{-}W_6(\mu_3\text{-}O)_6(\mu_3\text{-}Cl)_6Cl_6]^{2-}$ (**II**). It should be noted the synthesis of $[\alpha\text{-}W_6(\mu_2\text{-}O)_6(\mu_2\text{-}Cl)_6Cl_6]^{2-}$ published in [14] employed reduction of $WOCl_4$ with bismuth. We suppose that in our case $WCl_6$ contained some $WOCl_4$, because repetitive experiments, carried out under more meticulous protection from oxygen and moisture (freshly sublimed $WCl_6$, loading in a glovebox and thorough evacuation), led only to the salts of $[W_6Cl_{14}]^{2-}$ isolated as $Bu_4N^+$ (**I**), $H_3O^+$ (**III**) or $Cs^+$ (**IV**) salts. Crystals of $(H_7O_3)_2[W_6Cl_{14}]\cdot 3H_2O$ (**III**) were found isostructural to its molybdenum analogue [15]. Addition of pyridine to HCl solution, which contained $[W_6Cl_{14}]^{2-}$ and $[\alpha\text{-}W_6(\mu_3\text{-}O)_6(\mu_3\text{-}Cl)_6Cl_6]^{2-}$ led to precipitation of the $PyH^+$ salts. $(pyH)_2[W_6Cl_{14}]$ was identified by elemental analysis, whereas recrystallization of crude $(pyH)_2[\alpha\text{-}W_6(\mu_3\text{-}O)_6(\mu_3\text{-}Cl)_6Cl_6]$ resulted in partial substitution of four OH for bridging Cl and yielded an oxo-hydroxo-chloride bridged cluster $(pyH)_2[\alpha\text{-}W_6(\mu_2\text{-}OH)_4(\mu_2\text{-}O)_6(\mu_2\text{-}Cl)_2Cl_6]$ (**V**).

Cluster complex $(Bu_4N)_2[Mo_6Cl_8(CH_3COO)_6]$ (**VI**) was obtained from **I** by exchange reaction with silver perfluorobutyrate, driven by the formation of insoluble AgCl. Similar approach has been used for preparation of acetate and trifluoroacetate $(Bu_4N)_2[Mo_6Cl_8(CH_3COO)_6]$ and $(Bu_4N)_2[Mo_6X_8(CF_3COO)_6]$ (X = Cl, Br) complexes [16]. Complex **VI** is initially obtained as an oil, which crystallizes little by little. Its IR spectrum is typical for complexes with monodentate carboxylates. Bands at 1716 and 1366 $cm^{-1}$ refer to carboxylate group, while C–F bond appear at 1200–1100 $cm^{-1}$. Weak bands near 500 $cm^{-1}$ refer to W–O bond vibrations.

In a previous work [10] we studied reaction of $[(Mo_6Cl_8)Cl_6]^{2-}$ with $H_2Se$ generated in situ from ZnSe and 4M HCl at 140°C in molar ratios cluster/ZnSe from 1 : 3 up to 1 : 20. Subject to the reagents ratio, substitution of one or two chloride bridges by selenide occurs. In the case of $[(W_6Cl_8)Cl_6]^{2-}$ the reaction was carried out under the same conditions and was followed by ESI–MS technique, after precipitation of a possible mixture of anionic clusters with $Bu_4N^+$. Recrystallization of the crude precipitate yielded two types of crystals. Orange-red crystals belonged to the $(Bu_4N)_2[(W_6X_8)Cl_6]$ type [13]. Refinement of the statistic ratio Se/Cl in the X bridging positions could give no information about the amount of selenium. However, according to the ESI–MS(–) data the crystals contained a mixture of monoselenide derivative $[(W_6SeCl_7)Cl_6]^{2-}$ as well as original $[W_6Cl_{14}]^{2-}$ in approximately 2 : 1 molar ratio. Thus under similar conditions the tungsten cluster $[W_6Cl_{14}]^{2-}$ was turned out more inert to the insertion of a chalcogen into the cluster core than $[Mo_6Cl_{14}]^{2-}$, and the reaction stops already at the first stage. The reaction was also accompanied by one-electron oxidation of the 24-electron $\{W_6Cl_8\}^{4+}$ core into 23-electron $\{W_6SeCl_7\}^{4+}$ core. Assuming that crystals contain 2 : 1 molar mixture of $[W_6Cl_{14}]^{2-}$ and $[W_6SeCl_{13}]$, the share of selenium in every position does not exceed 1/24 and cannot be reliably determined by X-ray analysis.

When developing a single-stage synthesis of $[W_6Br_{14}]^{2-}$ from tungsten and bromine in presence of NaBr we discovered, along with $Na_2[W_6Br_{14}]$ which was isolated by extraction in diglyme and structurally characterized as $[Na(diglyme)_2][W_6Br_{14}]$ (**VII**), the formation of a few single crystals of two side products containing tungsten in higher oxidation states, namely, $Na[W_6OBr_{18}]$ (**VIII**) and $Na[W_6Br_{14}]$ (**IX**) characterized by X-ray analysis.

**Crystal structures.** All the complexes described in this paper contain cluster anions of four different types, their geometric characteristics presented in Table 2. Anions like $[W_6(\mu_3\text{-}X)_8X_6]^{2-}$ (X = Cl, Br) containing 24 cluster valence electrons (complexes **I**, **III**, **IV**, **VI**, **VII**) belong to the first type which contains octahedral cluster core held together by eight $\mu_3$-X bridging ligands besides direct W–W bonds. The rest of the tungsten coordination places are occupied by terminal halide (**I**, **III**, **IV**, **VII**; Fig. 1) or carboxylate (**VI**; Fig. 2) ligands. Average W–W distances are 2.610 Å (**I**), 2.614 Å (**IV**), 2.606 Å (**VI**), 2.635 Å (**VII**), being in a good agreement with the values reported for other salts of these anions.

**Table 2.** Average distances in the cluster cores of **I–IX**

| Complex | W–W(av) | W–$^{i}$X(av) | W–X(av) | W–O(av) | Reference |
|---|---|---|---|---|---|
| **I** | 2.610(1) | 2.497(5) | 2.426(5) | | This work, [14] |
| **II** | 2.9116(5)<br>2.6873(5) | 2.456(2) | 2.403(2) | 1.906(6) | » |
| **IV** | 2.614(3) | 2.506(8) | 2.428(8) | | » |
| **V** | 2.687(1)* | 2.457(2) | 2.403(1) | ** | » |
| **VI** | 2.606(1) | 2.500(1) | | 2.102(4) | » |
| **VII** | 2.635(1) | 2.6231(5) | 2.5889(5) | | » |
| **VIII** | 2.7246(3)<br>3.0018(3) | 2.5767(5)<br>2.5100(5) | 2.6339(5) | 2.17416(17) | » |
| **IX** | 2.6513(4) | 2.6119(9) | 2.5657(7) | | » |
| Ag[$W_6Br_{14}$] | 2.647(2) | 2.622(2) | 2.575(2) | | [18] |
| [$W_6Br_{14}$] | 2.653(1) | 2.608(1) | 2.569(1) | | [17] |
| $Cu_2[W_6Br_{14}]$ | 2.631(1) | 2.622(4) | 2.613(1) | | [20] |

* Data for short distances W–W.

** Distances W–O and W–OH have large distribution and are not shown.

Crystal structure of **I** and of the isostructural bromide cluster complex were determined earlier at room temperature. The authors chose a monoclinic cell setting, which can be reduced to our setting by rearrangement of *a* and *c* axes. Our data are in good agreement with literature values [13].

In the anionic cluster $[W_6Cl_8(C_3F_7COO)_6]^{2-}$ (**VI**) six perfluorobutyrate ligands coordinate to tungsten by oxygen atoms in monodentate way (Fig. 2), average W–O distances being 2.102 Å. The carboxylate groups of the perfluorobutyrate ligands coordinated to W(1) and W(2) are oriented in such a way that oxygen, carbon and tungsten atoms form a flat nine-link fragment resembling an open macrocycle (Fig. 3).

The second type includes $[W_6(\mu_3\text{-}Br)_8Br_6]^-$ anion **IX** (23 cluster valent electrons), which is oxidized form of $[W_6(\mu_3\text{-}X)_8X_6]^{2-}$ (24 cluster valence electrons). In the crystal structure the cluster anions are bonded in a 3D network by sodium cations (coordination number 6). According to the cell parameters, cubic **IX** is isostructural to the binary bromide [$W_6Br_{14}$] (22 cluster valence electrons) with molecular

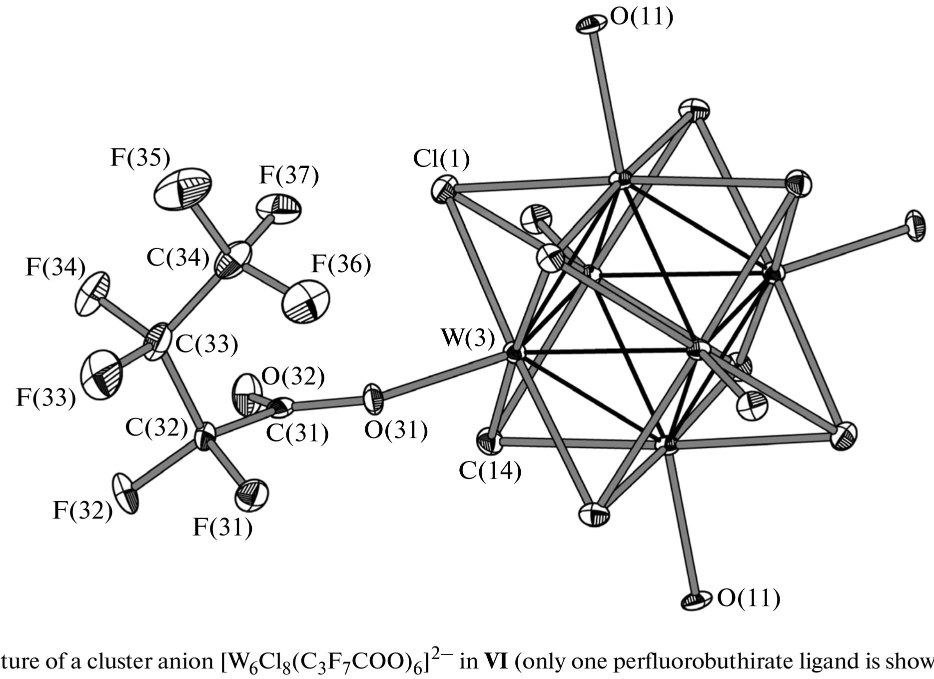

**Fig. 2.** Structure of a cluster anion $[W_6Cl_8(C_3F_7COO)_6]^{2-}$ in **VI** (only one perfluorobuthirate ligand is shown for clarity).

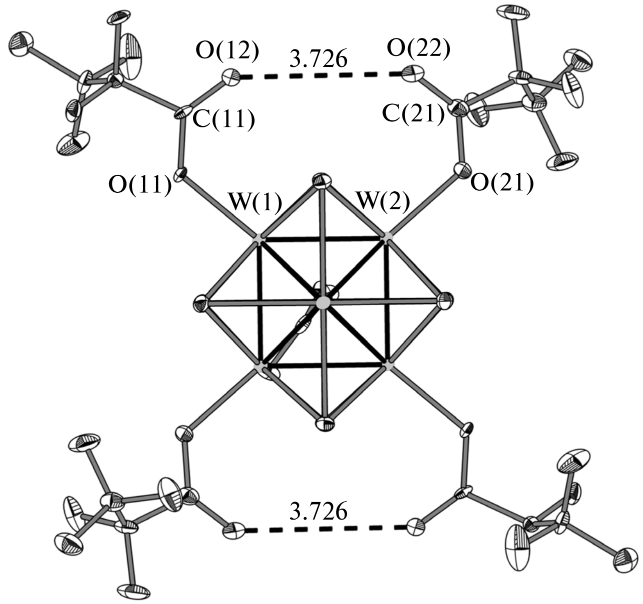

**Fig. 3.** Specific orientation of the perfluorobuthirate ligands in the crystal structure of **VI**.

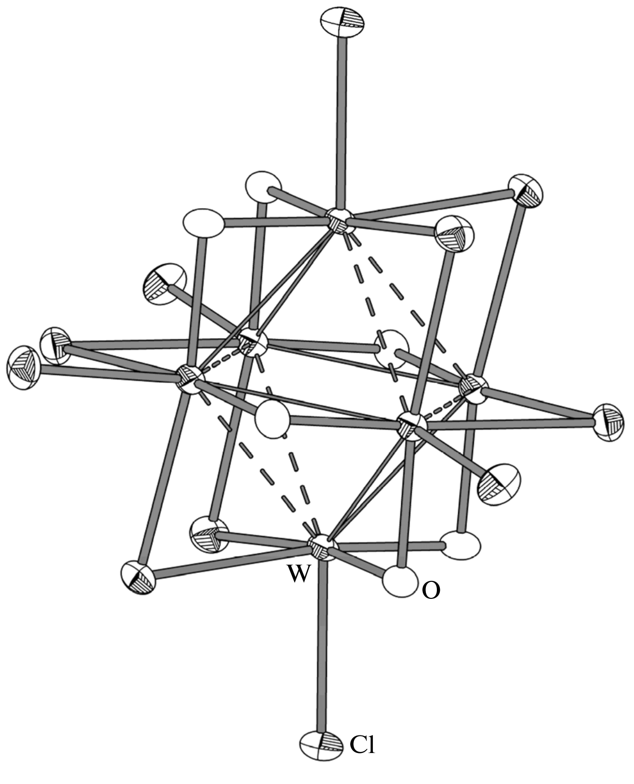

**Fig. 4.** Structure of a $[\alpha\text{-}W_6(\mu_2\text{-}O)_6(\mu_2\text{-}Cl)_6Cl_6]^{2-}$ (long metal-metal distances are in the dash style, short distances are in the solid style).

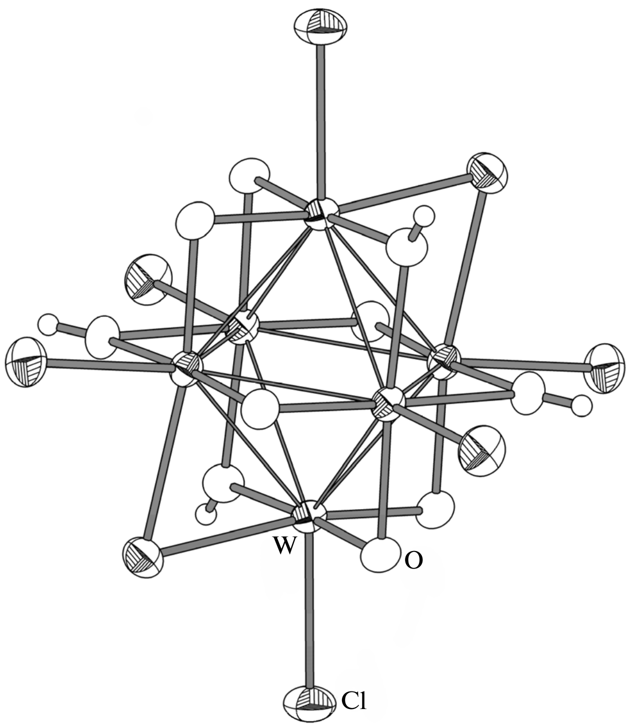

**Fig. 5.** Structure of a $[\alpha\text{-}W_6(\mu_2\text{-}OH)_4(\mu_2\text{-}O)_6(\mu_2\text{-}Cl)_2Cl_6]^{2-}$.

structure and face-centered cubic topology of cluster arrangement [17], and to $Ag[W_6Br_{14}]$ and $Pb[Mo_6Br_{14}]$ [18, 19]. Compound **IX** is also isotypic to $Cu_2[W_6Br_{14}]$ with three-coordinated $Cu^+$ [20]. Comparison of W–W and W–Br distances for 22, 23 and 24 electron clusters (Table 1) shows that increasing number of the cluster valence electrons shortens W–W bonds and lengthens both bridging and terminal W–Br bonds.

The third type comprises $[\alpha\text{-}W_6(\mu_2\text{-}O)_6(\mu_2\text{-}Cl)_6Cl_6]^{2-}$ (**II**) and $[\alpha\text{-}W_6(\mu_2\text{-}OH)_4(\mu_2\text{-}O)_6(\mu_2\text{-}Cl)_2Cl_6]^{2-}$ (**V**) (both with 14 cluster valence electrons) which belong to the rare for tungsten cluster type $[M_6(\mu_2\text{-}X)_{12}X_6]^{n-}$, more typical for Nb or Ta [21, 22]. Tungsten atoms form a distorted octahedron and bonded with twelve $\mu_2$-bridging ligands. The remaining coordination places are occupied by six terminal chloride ligands. Depending on the location of oxygen atoms the oxo-chloride clusters may be isolated in α or β isomeric forms [14]. Structure of $[\alpha\text{-}W_6(\mu_2\text{-}OH)_4(\mu_2\text{-}O)_6(\mu_2\text{-}Cl)_2Cl_6]^{2-}$ is shown in Fig. 4 (shorter and longer metal-metal distances are shown with lines of different thickness). Considering only stronger W–W interactions (2.685(1)–2.689(1) Å) the cluster core of **II** can be described as a metal-cyclohexane fragment in chair conformation with weaker additional interactions (2.908(1)–2.919(1)). In hot solutions partial substitution of only four of the six bridging chloride ligands leads to the formation of $[\alpha\text{-}W_6(\mu_2\text{-}OH)_4(\mu_2\text{-}O)_6(\mu_2\text{-}Cl)_2Cl_6]^2$ (**IV**) (Fig. 5) complex takes place. The W–O bonds for bridging hydroxide and bridging oxide have distinctive differences in length: the W–OH distances are 2.024(1), 2.034(1) Å, while the W–O distances vary from 1.907(1) to 1.947(1) Å. The W–W distances fall within 2.688(1)–2.846(1) Å.

The fourth type of clusters contains hexanuclear anion $[W_6(\mu_6\text{-}O)(\mu_2\text{-}Br)_{12}Br_6]^-$ which is found $Na[W_6(\mu_6\text{-}O)(\mu_2\text{-}Br)_{12}Br_6]^-$ (**VIII**) (16 cluster valence electrons) where tungsten atoms are placed in the vertexes of a triangular prism centered by a $\mu_6$-O ligand (Fig. 6). The tungsten atoms are bonded pairwise by bridging bromide ligands and the remaining coordination cites are occupied by terminal bromides. This is the first example of an oxygen-centered cluster among the tungsten clusters complementary to carbide and nitride-centered analogues (Table 3). In the crystal structure of **VIII** the cluster anions are bonded in a 3D network with sodium cations (coordination number 6), distances Na–Br are 2.9882(5) Å.

The dependence of W–W bond length from metal oxidation state has complicated character. Moreover direct comparison of M–M bond length for chloride and bromide clusters is incorrect dealing with known effect of lengthening of M–M bonding due to increasing of halogen radius (matrix effect of halogen). Unfortunately our attempts for “excision” of a cluster by melting with $NBu_4Br$ or by the diglyme extraction were not successful. Final solutions had intensive blue color and only salts of known anions $[WOBr_4]^-$ or *trans*-$[WOBr_4(H_2O)]^-$ were isolated.

In the structure of **VIII** the distances between tungsten atoms with the same triangular face appear shorter (2.7246(3) Å) than between the triangular faces (3.0018(3) Å). The distance between tungsten and the central oxygen lengthens only a little (2.17416(17) Å) in comparison with the carbide and nitride analogues.

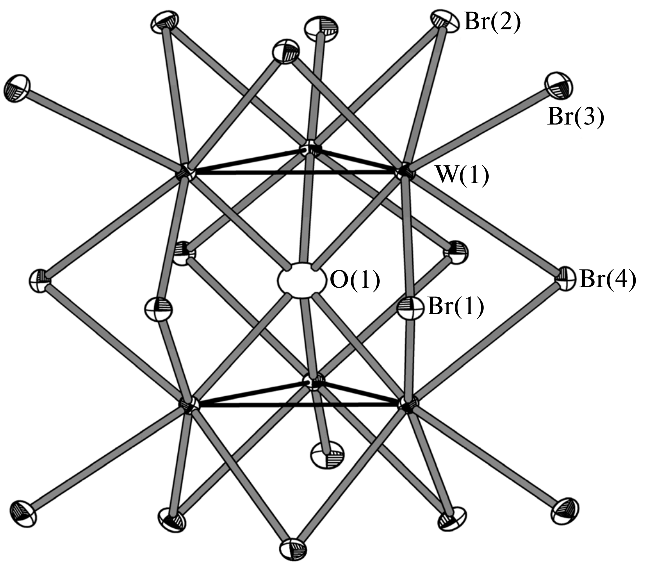

**Fig. 6.** Structure of a cluster anion $[W_6(\mu_6\text{-}O)(\mu_2\text{-}Br)_{12}Br_6]^-$.

In order to analyze packing motifs in the $[M_6X_{14}]^{2-}$ salts and related compounds we have concentrated on anion placement topology. Quantitative characteristics as coordination sequences and Schlaefli symbols which allow independent determination of packing motifs were calculated with TOPOS 4.0 Professional program complex [11]. For data interpretation mathematical apparatus developed for analysis of the pack-

**Table 3.** Main parameters of prismatic-type W complexes*

| Complex | +z | Y | W–Y$_{av}$, Å | W–W, Å | W3–W3, Å | Reference |
|---|---|---|---|---|---|---|
| $[W_6NCl_{18}]^-$ | 3.33 | N | 2.1682 | 2.6518(6) | 3.0705(7) | [23] |
| $[W_6NCl_{18}]^{2-}$ | 3.17 | N | 2.173 | 2.6574(6), 2.6608(6), 2.6585(6), 2.6584(6), 2.6759(6), 2.6835(6) | 3.0708(6), 3.0789(6), 3.0518(6) | [23] |
| $[W_6NCl_{18}]^{3-}$ | 3.00 | N | 2.16 | 2.606(1), 2.730(1), 2.732(1), 2.592(1), 2.740(1) | 3.087(1), 3.104(1), 2.803(1) | [23] |
| $[W_6CCl_{18}]^-$ | 3.50 | C | 2.157(8) | 2.74(1) | 2.93(2) | [24] |
| $[W_6CCl_{18}]^{2-}$ | 3.33 | C | 2.1595 | 2.66(7) | 3.028 | [24] |
| $[W_6CCl_{18}]^{3-}$ | 3.17 | C | 2.15(3) | 2.71(5) | 2.96(8) | [24] |
| $[W_6CCl_{12}(CF_3SO_3)_6]^{2-}$ | 3.33 | C | 2.15(3) | 2.632(2) | 3.037(5) | [25] |
| $[W_6CCl_{12}(Dmf)_6]^{2+}$ | 3.33 | C | 2.1323 | 2.6618 | 2.9562 | [25] |
| $[W_6CCl_{12}(Py)_6]^{2+}$ | 3.33 | C | 2.15(2) | 2.67(3) | 3.00(6) | [25] |
| $[W_6OBr_{18}]^-$ (**VIII**) | 3.17 | O | 2.174(1) | 2.725(1) | 3.002(1) | This work |

* *z*—average oxidation state of tungsten, Y—inner atom, W–W—d(W–W) in the triangular faces, W3–W3 = d(W–W) between tungsten triangles.

**Table 4.** Characteristics of the crystal packing of the anions in the salts of $[M_6X_{14}]^{2-}$ and related complexes

| Complex | Topology of anion sublatice | $G_3$ | $G_3^*$, % | Reference |
|---|---|---|---|---|
| $(Bu_4N)_2[W_6Cl_{14}]$ (**I**) | fcc | 0.07894 | 99.8 | This work |
| $(Bu_4N)_2[W_6O_6Cl_{12}]$ (**II**) | fcc | 0.07917 | 99.5 | " |
| $Cs_2[W_6Cl_{14}] \cdot 0.63H_2O$ (**IV**) | hcp | 0.07901 | 99.4 | " |
| $(PyH)_2[W_6(\mu\text{-}OH)_4(\mu\text{-}O)_6(\mu\text{-}Cl)_2)Cl_6] \cdot 4H_2O$ (**V**) | fcc | 0.08014 | 98.3 | " |
| $(Bu_4N)_2[W_6Cl_8(C_3F_7COO)_6]$ (**VI**) | fcc | 0.08142 | 96.7 | " |
| $(Na\{diglyme\}_2)_2[W_6Br_{14}]$ (**VII**) | fcc | 0.08439 | 93.3 | " |
| $Na[W_6(\mu_3\text{-}O)Br_{18}]$ (**VIII**) | hcp | 0.07959 | 98.7 | " |
| $Na[W_6Br_{14}]$ (**IX**) | fcc | 0.07875 | 100 | " |
| $(Bu_4N)_2[W_6Cl_{14}]$ | fcc | 0.07892 | 99.8 | [13] |
| $(Bu_4N)_2[W_6Br_{14}]$ | fcc | 0.07897 | 99.7 | [13] |
| $(Bu_4N)_2[W_6I_{14}]$ | fcc | 0.08065 | 97.6 | [13] |
| $(H_3O)_2[W_6Br_{14}] \cdot 4H_2O$ | hcp | 0.08020 | 97.9 | [28] |
| $[W_6Br_{14}]$ | fcc | 0.07875 | 100 | [17] |
| $Ag_2[W_6Br_{14}]$ | hcp | 0.07903 | 99.4 | [18] |
| $\alpha\text{-}Cu_2[W_6Br_{14}]$ | fcc | 0.07875 | 100 | [29] |
| $\beta\text{-}Cu_2[W_6Br_{14}]$ | fcc | 0.07875 | 100 | [29] |
| $Cd[W_6Br_{14}]$ | fcc | 0.07875 | 100 | [30] |
| $K_2[W_6Br_{14}]$ | fcc | 0.07875 | 100 | [31] |
| $Rb_2[W_6Br_{14}]$ | hcp | 0.08148 | 96.4 | [31] |
| $Cs_2[W_6Br_{14}]$ | hcp | 0.07894 | 99.5 | [31] |
| $Tl_2[W_6Br_{14}]$ | fcc | 0.07875 | 100 | [32] |

ing in monomolecular and ionic compounds was used [26, 27].

Results of crystal packing characteristics calculation are listed in Table 4. The $G_3^*$ parameter shows evenness of anion distribution (larger $G_3^*$ value means more even distribution), 100% being a value expected for the ideal structure of this type. As can be seen from Table 4, the principle of anionic close-packing is obeyed in every case. In other words, the topology of anionic centers of gravity always corresponds to fcc or hcp types. High values of $G_3^*$ indicate high evenness of the anionic substructures (negligible distortion). The most distorted substructures are those with asymmetric cations like $[Na(diglyme)_2]^+$ or large organic substituents coordinated to the cluster core.

It appeared interesting to examine the principle of close packing vs. an effect of possible presence anion-anion contacts in the structure. In the case of monoatomic cations like $Na^+$, $K^+$, $Tl^+$, etc., the anions contact with each other in all directions, forming a pseudo 3D framework with the cations occupying interstitial spaces. However in the structures with organic cations the latter efficiently shield anions from each other causing decrease in the network (pseudo)dimension down to 2D in $(Bu_4N)_2[W_6I_{14}]$, 1D in **II** and **VII**, or even to complete isolation of the anion by bulky $Bu_4N^+$ in **I** and isostructural $(Bu_4N)_2[W_6Br_{14}]$.

These observations show that cation-anion interactions and associated demands for accessible space and coordination environment can determine mutual orientation, but not the motif of gravity centers arrangement. Even isolation of anions by bulky organic cations cannot prevent close-packing arrangement of their substructure.

Authors thank Dr. C. Vicent (University Jaume I, Castellon, Spain) for recording ESI–MS spectra. The authors also thank Prof. V.A. Blatov (Samara State University) for kindly granting the TOPOS 4.0 Professional program. The work supported by State contract no. 14.740.11.0273 of Federal Program "Scientific and Scientific-Educational Personnel of Innovation Russia."

## REFERENCES

1. Fedorov, V.E., Mironov, Yu.V, Naumov, N.G., et al., *Usp. Khim.,* 2007, no. 76, p. 529.
2. Prokopuk, N. and Shriver, D.F., *Adv. Inorg. Chem.*, 1999, vol. 46, p. 1.
3. Tobola, J., Pecheur, P., Scherrer, H., et al., *J. Phys.: Condens. Matter*, 2003, vol. 15, no. 44, p. L655.

4. Chevrel, R., Gougeon, P., Potel, M., et al., *J. Solid State Chem.*, 1985, vol. 57, no. 1, p. 25.
5. Chevrel, R., Hirrien, M., and Sergent, M., *Polyhedron,* 1986, vol. 5, no. 1, p. 87.
6. Perrin, A., Perrin, C., and Sergent, M., *J. Less-Common Met.*, 1988, vol. 137, nos. 1–2, p. 241.
7. Nocera, D.G. and Gray, H.B., *J. Am. Chem. Soc.*, 1984, vol. 106, no. 3, p. 824.
8. Hilsenbeck, S.J., Young, V.G., and McCarley, R.E., *Inorg. Chem.,* 1994, vol. 33, no. 9, pp. 1822–1832.
9. Ebihara, M., Toriumi, K., and Saito, K., *Inorg. Chem.,* 1988, vol. 27, no. 1, p. 13.
10. Sokolov, M., Abramov, P., Virovets, A., et al., *J. Clust. Sci.*, 2009, vol. 20, p. 83.
11. Blatov, V.A., http://www.iucr.org/iucr-top/comm/ccom/newsletters
12. Kolesnichenko, V. and Messerle, L., *Inorg. Chem.,* 1998, vol. 37, p. 3660.
13. Zietlow, T.C., Schaefer, W.P., Sedeghi, B., et al., *Inorg. Chem.,* 1986, vol. 25, p. 2195.
14. Crawford, N.R.M. and Long, J.R., *Inorg. Chem.,* 2001, vol. 40, p. 3456.
15. Flemstroem, A., Hirsch, T.K., Sehlstedt, L., et al., *Solid State Sciences*, 2002, vol. 4, p. 1017.
16. Sokolov, M.N., Mihailov, M.A., Peresypkina, E.V., et al., *Dalton Trans.,* 2011, vol. 40, no. 24, p. 6375.
17. Sassmannshausen, J. and von Schnering, H.G., *Z. Anorg. Allg. Chem.*, 1994, vol. 620, p. 1312.
18. Zheng, Y.-Q. and von Schnering, H.G., *Z. Anorg. Allg. Chem.*, 1999, vol. 625, p. 2115.
19. Boeschen, S. and Keller, H.L., *Z. Kristallogr.,* 1992, vol. 200, p. 305.
20. Ihmaine, S., Perrin, C., and Sergent, M., *Eur. J. Solid State Inorg. Chem.*, 1997, vol. 34, p. 169.
21. Koknat, F.W., Parsons, J.A., and Vongvusharintra, A., *Inorg. Chem.,* 1974, vol. 13, p. 1699.
22. Hughes, B.G., Meyer, J.L., Fleming, P.B., et al., *Inorg. Chem.,* 1970, vol. 9, p. 1343.
23. Welch, E.J., Yu, C.L., Crawford, N.R., and Long, J.R., *Angew. Chem.,* 2005, vol. 117, p. 2605.
24. Welch, E.J., Crawford, N.R., Bergman, R.G., and Long, J.R., *J. Am. Chem. Soc.*, 2003, vol. 125, p. 11464.
25. Welch, E.J. and Long, J.R., *Angew. Chim. Int. Ed.*, 2007, vol. 46, no. 19, p. 3494.
26. Peresypkina, E.V. and Blatov, V.A., *Acta Crystallogr., Sect. B: Struct. Sci.*, 2000, vol. 56, p. 501.
27. Peresypkina, E.V. and Blatov, V.A., *Acta Crystallogr., Sect. B: Struct. Sci.*, 2000, vol. 56, 1035.
28. Yarovoi, S.S., Tarasenko, M.S., Brylev, K.A., et al., *Russ. J. Coord. Chem.*, 2012, vol. 38, no. 6, p. 402.
29. Zheng, Y.Q., Grin, Y., Peters, K., et al., *Z. Anorg. Allg. Chem.*, 1998, vol. 624, no. 6, p. 959.
30. Ihmaine, S., Perrin, C., and Sergent, M., *Croat. Chem. Acta*, 1995, vol. 68, no. 4, p. 877.
31. Zheng, Y.Q., Peters, K., Grin, Y., et al., *Z. Anorg. Allg. Chem.*, 1998, vol. 624, no. 3, p. 506.
32. Zheng, Y.Q., Peters, K., and von Schnering, H.G., *Z. Kristallogr.-New Cryst. Struct.*, 1998, vol. 213, no. 4, p. 681.